Space-Charge-Limited 2D Electron Flow between Two Flat Electrodes in a Strong Magnetic Field

A. Rokhlenko and J. L. Lebowitz*

Department of Mathematics, Rutgers University, Piscataway, New Jersey 08854-8019, USA

(Received 15 October 2002; revised manuscript received 18 February 2003; published 19 August 2003)

An approximate analytic solution is constructed for the 2D space-charge-limited emission by a cathode surrounded by nonemitting conducting ledges of width Λ. An essentially exact solution (via conformal mapping) of the electrostatic problem in vacuum is matched to the solution of a linearized problem in the space charge region whose boundaries are sharp due to the presence of a strong magnetic field. The current density growth in a narrow interval near the edges of the cathode depends strongly on Λ. We obtain an empirical formula for the total current as a function of Λ which extends to more general cathode geometries.

DOI: 10.1103/PhysRevLett.91.085002 PACS numbers: 52.27.Jt, 52.59.Sa, 52.59.Wd, 85.45.Bz

The study of space-charge-limited current (SCLC), initiated in the beginning of the last century [1,2], continues to be of great current interest [3–9]. These works are important for the design of high power diodes, techniques of charged particles beams, physics of non-neutral plasmas including plasma sheath, and other numerous applications. The modeling of SCLC of ions in cylindrical and spherical geometry [3] is also necessary for the inertial-electrostatic confinement of fusion plasmas. Unfortunately only the planar 1D case permits an analytic solution [1,2] and, as pointed out in a recent review [5], even "the seeming simple problem of 2D planar emission remains unresolved."

This motivated the present work which provides a semianalytic solution for a prototype 2D model similar to that studied in [6]. The novel feature of our approach is the explicit analysis of the electric fields at the interface between the current region and the vacuum which create the spikes of the current density. This differs from previous computations [5,6,8] where the problem was solved numerically by computing electron trajectories without proper treatment of the vacuum fields. We obtain for the first time, we believe, a reasonable analytic approximation for these spikes (current wings)—an important (though usually undesirable) feature of SCLC diodes [6,7]. An extension of our methods should facilitate dealing with this problem in more general SCLC situations.

Model.—We consider the current between two conducting flat electrodes where the anode, whose potential is V, is an infinite plane separated by a distance D from the grounded cathode which is an infinitely long strip parallel to the anode. Our assumptions are (i) the cathode upper surface, of width $2A$, has infinite emissivity while the lower face and the ledges of widths Λ do not emit (see Fig. 1); (ii) a strong magnetic field perpendicular to the electrodes inhibits the transversal components of electron velocities [6,8], but almost does not affect the total current [6,8,9]; (iii) the emitted electrons leave the cathode with zero velocity [1,2,6].

If the cathode is in the (X, Z) plane and the magnetic field in the Y direction, the velocities v of electrons are parallel to the Y axis with $mv^2(X, Y) = 2eU(X, Y)$, where $U(X, Y)$ represents the potential field while m, e are the electron mass and charge. The current density $J(X)$, which clearly is Y independent, determines together with $v(X, Y)$ the density of electrons. Using the dimensionless variables $x = X/D$, $y = Y/D$, $a = A/D$, $\lambda = \Lambda/D$, in which D is the unit of length, and $\phi(x, y) = U(X, Y)/V$, $j(x) = 9\pi D^2 V^{-3/2}(m/2e)^{1/2} J(X)$, the nonlinear Poisson equation for the potential then takes the form

$$\frac{\partial^2 \phi}{\partial x^2} + \frac{\partial^2 \phi}{\partial y^2} = -4\pi\rho(x, y) = \frac{4j(x)}{9\sqrt{\phi(x, y)}}. \tag{1}$$

The electron density $\rho(x, y)$ and current $j(x)$ are different from zero only in the shaded rectangle Q of Fig. 1 which shows a two-dimensional cross section of our system.

The x components of the electric field near $x = \pm a$ will drive the electrons and smear the vertical boundaries of Q. Our method requires the Larmor radii of electrons to be small, say 5% of D. A magnetic field 1 kG is sufficient when $D \sim 1$ cm and $U < 10$ kV.

Equation (1), subject to the boundary conditions (BC),

$$\begin{aligned} &\phi(x, 0) = 0 \quad \text{for } |x| < a + \lambda, \\ &\phi(x, 1) = 1 \quad \text{for } |x| < \infty, \\ &\frac{\partial \phi}{\partial y}(x, +0) = 0 \quad \text{for } |x| < a, \end{aligned} \tag{2}$$

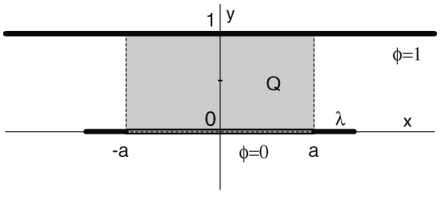

FIG. 1. Geometry of the system.

is to be solved in the half-plane $y \leq 1$ to produce both functions $\phi(x, y)$ and $j(x)$ which are non-negative and symmetric about the y axis. To do this we first solve Eq. (1) approximately in the current region Q on a rather intuitive level. The problem is nonlinear here and it is not well posed if one disregards the field at $|x| > a$. Consequently our solution will have a set of free parameters which specify $j(x)$ and $\phi(x, y)$. In the second step the potential $\phi(\pm a, y)$ is used as the BC and we obtain a Dirichlet problem for the Laplace equation (1) in the outer region of the half-plane where $j(x) = 0$. We solve this problem using conformal mapping techniques and evaluate $\frac{\partial \phi}{\partial x}(a^+, y)$. If one excludes the points $x = \pm a, y = 0$ the electron density $\rho(a^-, y)$ is finite and $\rho(a^+, y) = 0$; therefore the second derivative of $\phi(x, y)$ has a finite jump at $x = a$, while the first derivative must be continuous, i.e.,

$$\frac{\partial \phi}{\partial x}(a^-, y) = \frac{\partial \phi}{\partial x}(a^+, y), \qquad 0 < y < 1. \tag{3}$$

In the last step we satisfy approximately the matching condition (3) by adjusting the free parameters mentioned above using the least squares technique. This will give an approximate explicit form for $j(x)$.

The space charge region Q.—We want to solve approximately Eq. (1) where the function $j(x)$ is not known nor are the BC for ϕ at $x = \pm a$. When $a = \infty$ we have no x dependence and (1) becomes an ordinary equation which was solved in [1,2] yielding $\phi_1(y) = y^{4/3}, j_1(x) = 1$. This gives the Child-Langmuir formula [1], $J_1 = (2e/m)^{1/2} V^{3/2}/9\pi D^2$. For $a \gg 1$ it is reasonable to assume that $j(x) \sim j_1 = 1$ when $a - |x| \gg 1$ and use also a stronger assumption that the difference $\phi(x, y)/\phi_1(y) - 1$ is small almost everywhere (i.e., it does not exceed $\sim$1–1.5 even near the edges of region). This difference, however, is not small at the cathode edges, $x = \pm a$, where the electric field must match the field outside. The large gradients in the field lead to the acceleration of electrons and thus to a strong rise of the current density $j(x)$ near the boundary of the SCLC.

We represent $\phi(x, y)$ in the form $y^{4/3}[1 + \mu(x, y)]$ and linearize the square root as $[1 + \mu(x, y)]^{-1/2} \approx 1 - \beta\mu(x, y)$, where the number β is chosen to minimize the integral of $[1 - \beta\mu - (1 + \mu)^{-1/2}]^2$ on the interval $0 \leq \mu \leq 1$. This yields $\beta \approx 0.328$ with relative average error of approximation around 2.2%. For $\mu = 0.2, 1, 1.5$ the error is 2.36%, 4.96%, 19.6%, respectively. We shall see later that for all $\lambda \geq 0.1$, $\mu < 1.5$. Substituting in (1) we obtain a linear equation

$$y^2\left(\frac{\partial^2 \mu}{\partial x^2} + \frac{\partial^2 \mu}{\partial y^2}\right) + \frac{8}{3} y \frac{\partial \mu}{\partial y} + 4\frac{1 + \beta}{9}\mu = \frac{4}{9}[j(x) - 1], \tag{4}$$

where we dropped a nonlinear term in the right-hand side. The error due to this and to the linearization of the square root is negligible for small μ and decreases the right-hand side by at most a factor $\sim$0.7, in all the cases considered (see Table I), including even $\mu \approx 2$.

Using the method of separation of variables we write

$$\mu(x, y) = \sum_l q_l f_l(x) u_l(y), \qquad j(x) = 1 + \frac{9}{4}\sum_l q_l f_l(x), \tag{5}$$

with

$$f_l(x) = e^{-k_l(a-x)} + e^{-k_l(a+x)}, \qquad |x| \leq a. \tag{6}$$

Substituting (5) and (6) into (4) and assuming that (4) and (2) are satisfied separately for each $l = 1, 2, \ldots$ gives a set of inhomogeneous equations

$$y^2 \frac{d^2 u_l}{dy^2} + \frac{8}{3} y \frac{du_l}{dy} + \left(k_l^2 y^2 + 4\frac{1 + \beta}{9}\right) u_l = 1, \tag{7}$$

with the common BC $u_l(1) = 0$. The parameters k_l and q_l will be determined later. The potential can be written in the form

$$\phi(x, y) = y^{4/3} + y^{4/3} \sum_l q_l f_l(x) u_l(y), \tag{8}$$

where the first term is the Child-Langmuir potential ϕ_1 and the $u_l(y)$ are assumed finite. The relevant particular solutions of (7), which can be expressed in terms of Lommel's functions $s_{-1/6,\nu}(k_l y)$, $\nu = \sqrt{9 - 16\beta}/6$ [10], are given by the power series expansion

$$u_l(y) = \frac{9}{4(1 + \beta)} \sum_{n=0}^{\infty} (-1)^n a_n \left(\frac{k_l y}{2}\right)^{2n}, \qquad a_0 = 1,$$
$$a_n = \frac{a_{n-1}}{n^2 + 5n/6 + (1 + \beta)/9}. \tag{9}$$

As all $u_l(1) = 0$ the parameters k_l are the increasing roots of (9): 3.881, 6.675, 10.065, 13.003, 16.316, 19.306, 22.582, 25.600, 28.855, 31.891 for $1 \leq l \leq 10$. They can be easily evaluated due to the rapid convergence of (9), asymptotically $k_l \to l\pi$. The free parameters q_l will be used to satisfy (3).

TABLE I. Results of computations.

λ	0	0.1	0.3	0.5	1	∞
α	0.6487	0.5311	0.3463	0.2665	0.2067	0.1905
$\mu_{\max}$	1.955	1.432	0.804	0.605	0.497	0.461
$j_{\max}$	3.597	2.902	2.068	1.804	1.661	1.612
Δ	0.0121	0.0055	0.0037	0.0028	0.0059	0.0044
q_1	0.2448	0.2339	0.1891	0.1530	0.1140	0.1032
q_2	0.2225	0.1743	0.0926	0.0616	0.0465	0.0443
q_3	0.1867	0.1411	0.0720	0.0528	0.0448	0.0433
q_4	0.1525	0.0969	0.0389	0.0280	0.0260	0.0246
q_5	0.1184	0.0760	0.0327	0.0253	0.0232	0.0222
q_6	0.0914	0.0500	0.0192	0.0143	0.0148	0.0134
q_7	0.0595	0.0342	0.0142	0.0110	0.0109	0.0100
q_8	0.0439	0.0216	0.0087	0.0061	0.0072	0.0061
q_9	0.0203	0.0108	0.0046	0.0033	0.0037	0.0032
q_{10}	0.0142	0.0064	0.0028	0.0017	0.0025	0.0019

The 2D mean current density over the whole cathode, which in terms of our scheme is given by

$$j_2 = \frac{1}{a}\int_0^a j(x)dx \approx 1 + \frac{9}{4a}\sum_l \frac{q_l}{k_l}(1 - e^{-2k_l a}), \quad (10)$$

is usually presented [8] as the 1D current density $j_1 = 1$ plus a correction: $j_2 = 1 + \alpha/2a$. Thus in the original units the mean current has the form

$$J_2 = J_1\left(1 + \alpha\frac{D}{W}\right), \quad (11)$$

where $W = 2A$ is the width of the cathode. Using (10) the parameter α is defined here by

$$\alpha = 9\sum_l \frac{q_l}{2k_l}(1 - e^{-2k_l a}). \quad (12)$$

Electrostatic region.—It seems clear that for $a \gg 1$ the electric field in the vicinity of the boundary $x \approx a, 0 \le y \le 1$ is not affected much by the region $x \le -a, 0 \le y \le 1$; see Fig. 1. This allows us to study a simpler electrostatic problem for a plane which is split according to Fig. 2(a). We modified a conformal transform in [11] to the form

$$z = 2\pi^{-1}[\ln(\sqrt{w} + \sqrt{w-1}) - c\sqrt{w^2 - w}], \quad (13)$$

which maps the shaded half-plane $z = x + iy$ on Fig. 2(a) onto the upper half-plane $w = u + i\upsilon$ in Fig. 2(b).

Our Dirichlet problem with the BC on the real axis $\Im w = 0$ (which come from the previous section),

$$\Phi(u, 0) = \begin{cases} 1, & \text{if } -\infty < u \le 0, \\ \phi(a, y(u)), & \text{if } 0 < u < 1, \\ 0, & \text{if } u \ge 1, \end{cases} \quad (14)$$

has the solution

$$\Phi(u, \upsilon) = \frac{\upsilon}{\pi}\int_{-\infty}^{\infty} \frac{\Phi(s, 0)}{(u - s)^2 + \upsilon^2} ds \quad (15)$$

in the upper half-plane w. Here by (13) $y(u) = 2\pi^{-1}[\arccos\sqrt{u} - c\sqrt{u(1-u)}]$. The potential $\Phi(u, \upsilon)$ expressed in variables x, y represents $\phi(x, y)$ outside the space charge zone. Our task now is to match the inside electric field $\frac{\partial\phi}{\partial x}(a, y(u))$ in the interval $0 < u < 1$ with the field outside

$$\frac{\partial\Phi}{\partial x}(u, \upsilon = 0) = \frac{\pi\sqrt{u(1-u)}}{1 + c(1-2u)}\frac{\partial\Phi}{\partial\upsilon}(u, 0). \quad (16)$$

Continuity of the electric field.—The matching condition (3) guarantees continuity of the electric field at the boundary between the space charge region Q with the vacuum. Using (6) and (8) we have at $x = a$ inside the space charge region the field intensity,

$$\frac{\partial\phi}{\partial x} = y^{4/3}\sum_l q_l k_l (1 - e^{-2k_l a})u_l(y), \quad (17)$$

which should be equal to the vacuum field (16). The exponentially small terms $e^{-2k_l a}$ can be dropped as a is assumed large. Both terms $\frac{\partial\phi}{\partial x}$ and $\frac{\partial\Phi}{\partial x}$ depend on all parameters q_l, but in a different way. One cannot expect an exact equality because of the approximations made. We rewrite the condition (3) as

$$G[y^{4/3}] + \sum_l q_l\{G[y^{4/3}u_l(y)] - k_l y^{4/3}u_l(y)\} \approx 0, \quad (18)$$

where the functionals G can be written explicitly as integrals with a logarithmic singularity.

We minimize the least square divergence from zero of the expression (18) on the interval $0.15 < y < 0.85$ without approaching the end points where our treatment is not entirely adequate. A standard procedure yields a set of linear algebraic equations for q_l. We did not go further than $l_{\max} = 10$. After the q_l are computed one can find the current density (5) and the parameter α (12).

The accuracy of this method can be evaluated to some degree by determining the relative average discrepancy Δ of matching the BC in (3). The results of our computations are shown in the Table I, where for different values of the ledge λ one can see also $\alpha(\lambda)$, parameters q_l, $\mu_{\max}$ (near $y = 0$ and $x = \pm a$), and the relative height (see Fig. 3) of the current wings $j_{\max}$ at $x = \pm a$. When we extend the interval of matching the electric fields up to $(0.01, 0.99)$ the quantities in the table stay approximately the same, only Δ increases. This confirms the general validity of our method and simultaneously shows that the computation of electric fields near the corners of the rectangle Q is not very good. In particular, in the worst case (the most severe cathode regime; see also [6,7,12]) when $\lambda = 0$, the electric field is singular at the cathode edges. The computation becomes unstable and the corresponding data of Table I are not reliable.

When l runs from one to ten, the values of q_l decrease approximately by a factor 20–50. Therefore, parameter α

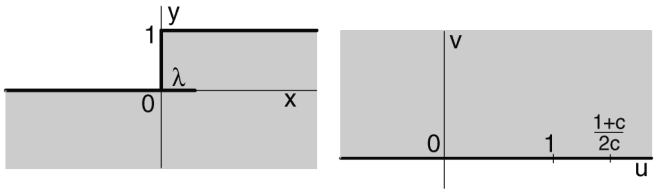

FIG. 2. (a) Plane $z = x + iy$. (b) Plane $w = u + i\upsilon$.

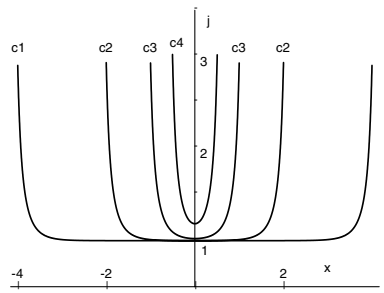

FIG. 3. The current densities when $\lambda = 0.1$, $c1 - c1$, $c2 - c2$, $c3 - c3$, and $c4$ correspond to $2a = 8, 4, 2, 1$, respectively.

even for $l_{\max} = 10$ is evaluated very well by (12) where the k_l increase from ~4 to 32. The accuracy of $j(x)$ and $\mu(x)$ might be improved if one truncates [8] at a larger $l_{\max}$ though we would not expect dramatic changes. The cases $\lambda = \infty$ (when the mapping is exact) and $\lambda = 1$ are very close, which means that the parameter $\alpha(a, \lambda)$ as well as q_l are approximately independent of a when $a > 1$ (the situation studied here). Keeping the exponential terms in $\mu(x, y)$ in the matching condition (17) does not complicate the calculation and it will give only insignificant corrections. The current density $j(x)$ at $x = 0$ increases in this case by about $2q_1 e^{-3.9a}$. If a is smaller, but $2(\lambda + a) > 1$, the scheme of computation is the same though the q_l become functions of a and one cannot decrease a too much because the first term in (8) needs corrections.

An important part of our analysis is the form (6) of $f_l(x)$ which implies that the current density (5) in a narrow region of width ~1 at the cathode edges has a sharp peak which decays faster than $\exp[-3.88(a - |x|)]$. Everywhere else, $j(x)$ is close to the 1D current $j_1(x) = 1$ with exponentially small corrections. Plots of the current density distribution (5) are shown in Fig. 3 for different widths of the cathode.

We can compare our curve $c3$ for $a = 1$ with particle-in-cell (PIC) simulations presented in [7]. There, for zero cathode recess ($dx = 0$), $A = 50$ mm, and unfortunately unspecified width of the shroud a reasonable fit would be $j_{\max} = 3.9$ in Table I for $\lambda = 0.1$ versus 3.2 in [7]. We get the half-width of the current density peak ~1.2 mm while in [7] it was 1 mm. Our magnetic field is stronger and we think also that PIC simulations with finer grids are closer to our computation, but diverge from experimental results because the real cathodes with their finite thickness and roundness do not have the very strong electric field intensities present, however, in the models.

Generalization..—We expect that this pattern of uniformly shaped narrow wings of the current density holds also for finite flat cathodes with perimeter P and area S (in original units) assuming $S \gg PD$, reasonable restrictions on the cathode curvature, and constant width of the non-emitting ledges. The boundary region will have an area $\sim PD$ and the total current can be written as the sum $I = SJ_1 + PD\tilde{J}$ where the "edge" current $\tilde{J}$ can be evaluated in terms of the parameter α defined in (12). Comparing $\bar{J} = I/S = J_1(1 + \tilde{J}PD/J_1S)$ with Eq. (11) for our geometry we have $\tilde{J} = J_1\alpha/2$ and finally

$$\bar{J} = J_1\left(1 + \alpha\frac{PD}{2S}\right), \tag{19}$$

which should be applicable in general situations. In particular, the factor $PD/2S$ in (19) becomes D/R for a circular cathode of the radius R and $2DE(\sqrt{1 - C^2/B^2})/\pi C$ for an elliptical cathode with the half-axes $B > C$, where $E(k)$ is the complete elliptical integral. For a rectangular cathode with the sides L and H it is equal to $D(L^{-1} + H^{-1})$.

Conclusions.—(i) The current wings, Fig. 3, resemble simulated wings [6,7,12]. They are high when the width of ledges λ is small and the vacuum electric field near the cathode edges is strong. Their form becomes practically constant when the ledges are wider than the distance D between electrodes. (ii) The shape of the current wings [see eigenvalues k_l of (7)] is roughly exponential and the 1D current is restored up to a few percent at the distance D from the edges. (iii) The parameter α, which defines the net current density, depends on the width of ledges. An approximate empirical formula

$$\alpha(\lambda) \approx 0.19 + 0.48e^{-3.7\lambda}, \tag{20}$$

agrees with the data in Table I within ~3.3%. (For a different model with the constant current density α was estimated in [8] as close to 0.31.) (iv) Our techniques of matching the electric fields at the boundary of the space charge region and using rather modest variations of the potential in the x direction are effective for approximate modeling the 2D and 3D flows of charged particles.

We thank R. Barker, R. J. Umstattd, and O. Costin for inspiration and useful comments. Research supported by AFOSR Grant No. F49620-01-0154.

*Also at Department of Physics, Rutgers University, Piscataway, NJ 08854-8019, USA.

[1] C. D. Child, Phys. Rev. **32**, 492 (1911); I. Langmuir, Phys. Rev. **2**, 450 (1913).

[2] I. Langmuir and K. B. Blodgett, Phys. Rev. **22**, 347 (1923); I. Langmuir and K. B. Blodgett, Phys. Rev. **24**, 49 (1924).

[3] D. C. Barnes and R. A. Nebel, Phys. Plasmas **5**, 2498 (1998); R. A. Nebel and D. C. Barnes, Fusion Technol. **38**, 28 (1998).

[4] A. S. Gilmour, Jr., *Microwave Tubes* (ArtechHouse, Dedham, MA, 1986); P. T. Kirstein, G. S. Kino, and W. E. Waters, *Space Charge Flow* (McGraw-Hill, New York, 1967); A. Valfells, D. W. Feldman, M. Virgo, P. G. O'Shea, and Y. Y. Lau, Phys. Plasmas **9**, 2377 (2002).

[5] J. W. Luginsland, Y. Y. Lau, R. J. Umstattd, and J. J. Watrous, Phys. Plasmas **9**, 2371 (2002).

[6] R. J. Umstattd and J. W. Luginsland, Phys. Rev. Lett. **87**, 145002 (2001).

[7] F. Hegeler, M. Friedman, M. C. Myers, J. D. Sethian, and S. B. Swanekamp, Phys. Plasmas **9**, 4309 (2002).

[8] J. W. Luginsland, Y. Y. Lau, and R. M. Gilgenbach, Phys. Rev. Lett. **77**, 4668 (1996); Y. Y. Lau, Phys. Rev. Lett. **87**, 278301 (2001).

[9] Y. Y. Lau, P. J. Christenson, and D. Chernin, Phys. Fluids B **5**, 4486 (1993).

[10] *Higher Transcendental Functions*, edited by A. Erdelyi (McGraw-Hill, New York, 1953), Vol. 2.

[11] W. von Koppenfelds and F. Stallmann, *Praxis der Konformen Abbildung* (Springer-Verlag, Berlin, 1959).

[12] R. J. Umstattd, D. A. Shiffler, C. A. Baca, K. J. Hendricks, T. A. Spencer, and J. W. Luginsland, Proc. SPIE Int. Soc. Opt. Eng. **4031**, 185 (2000).